

PAPER • OPEN ACCESS

Effect of Increased Density of Nodes in Geodesic Dome on its Critical Load Capacity

To cite this article: Pawel Zabojszcza and Urszula Radon 2019 *IOP Conf. Ser.: Mater. Sci. Eng.* **471** 052051

Recent citations

- [The Impact of Node Location Imperfections on the Reliability of Single-Layer Steel Domes](#)
Paweł et al

View the [article online](#) for updates and enhancements.

Effect of Increased Density of Nodes in Geodesic Dome on its Critical Load Capacity

Pawel Zabojszcza ¹, Urszula Radon ¹

¹ Kielce University of Technology, Al. Tysiaclecia Panstwa Polskiego 7,25-314
Kielce, Polska

zabojszcza.pawel@gmail.com

Abstract. The paper reports an attempt at assessing the effect of geodesic dome mesh refinement on the structure critical load capacity. The initial surface of geodesic domes is the sphere divided into spherical triangles. Consecutive divisions of the spherical triangles decide the mesh refinement of the geodesic domes. Two computational models (3V and 4V) were examined. For 4V dome, two types of structure, namely truss and frame ones were considered. For 4V frame system, the values of the critical load capacity were determined for three buckling lengths of the bars μ : 0.5, 0.7 and 1.0.

1. Introduction

Lattice domes are cyclically symmetric structures. They contain many struts of the same geometry; consequently, they are convenient from the standpoint of modern fabrication organisation and assembly. Popularity of steel lattice domes has been on the rise due to decidedly lower mass and shorter construction time compared with solid domes [1]. As regards lattice domes, a geodesic dome is one of the widely used structural solutions. The initial surface of geodesic domes is the sphere divided into spherical triangles. The geodesic sphere, based on icosahedron is actually commonly used in graphics application to approximate a sphere because of the minimum amount of information that is needed to create the polygon necessary. Consecutive divisions of the spherical triangles decide the mesh refinement of the geodesic domes.

Owing to the method of sphere division into spherical triangles, developed by Buckminster Fuller in 1954, geodesic domes gained in popularity. He patented two means of dome subdivision. The first solution involves connecting the centres of the sides of spherical triangle ABC with arcs of great circles. As a result, four spherical triangles are produced. Consecutive subdivisions follow the same pattern (figure 1a). In an alternative solution, three arcs of great circles of the spherical triangle ABC are drawn in such a way that they cross each side of the triangle at two points. Appropriately connecting numerals 1,2,3,4,5,6 (figure 1b) produces a spherical hexagon and three identical equilateral vertex triangles. Further subdivisions of triangles thus produced proceed in the same manner.

Interest in Fuller's domes has continued until the present day. Other arrangements in the subdivision of the spherical mesh of regular icosahedrons have been proposed. In one of the options, regular hexagons are produced, and also, regardless of the frequency, 12 regular pentagons located at the vertices of regular icosahedron.



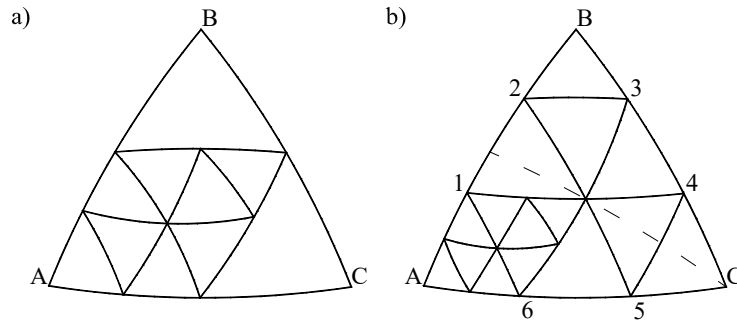


Figure 1. Two ways of subdivision of equilateral spherical triangle acc. the Fuller method

The advantages of such a structural solution for steel covers include, among others, minimisation of material use, of the area (approx. 30% lower than in conventional structures) or a low number of different struts, especially for small spans. Disadvantages involve a necessity of designing one-standard heating, or ventilation systems. That can result from the possibility of the occurrence of problems related to moisture condensation in the upper parts of the structure. Other difficulties concern technological issues such as installation of standard door and windows. However, geodesic domes are used as covers of the world's largest building. The examples include Fukuoka Dome, with a diameter of 222 meters, a baseball park in Japan and Louvre Abu Dhabi museum, with a diameter of approx. 180m, in the United Arab Emirates [2].

2. The Spherical-Coordinate System

The position of a point in three-dimensional space is clearly defined by three coordinates:

- (x, y, z) - in the Cartesian system,
- (r, θ, φ) - in a spherical system
- (ρ, φ, z) - in a cylindrical system (figure 2).

The coordinate system can be freely selected depending on the problem under consideration.

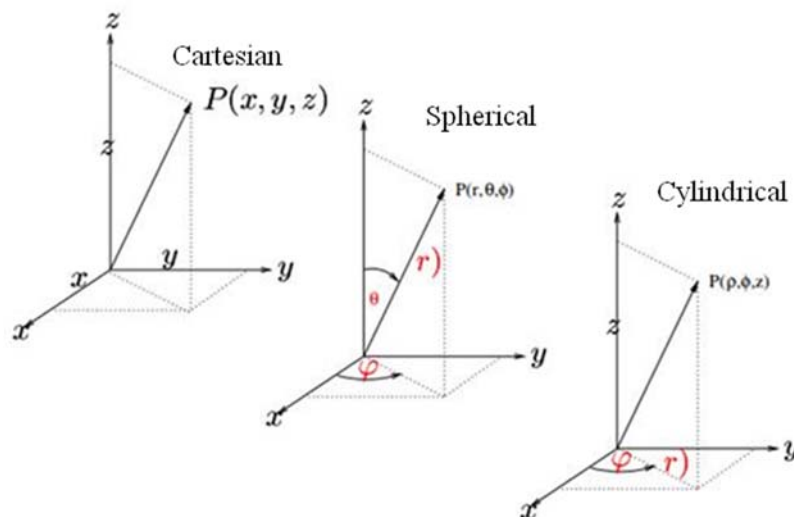


Figure 2. Spatial coordinate systems

The geometry of geodesic domes (spheres) is most conveniently described using a spherical coordinate system. Two angles θ and φ determine the direction and in combination with the distance r specify the position of the unique point in space. The φ coordinate resembles a meridian of

longitude. All points with the same φ lie on the same great circle, which passes through the zenith (0,0). It is convenient to incorporate the reference meridian $\varphi=0$ into calculations whenever it is possible. The first coordinate of all points situated on it will be zero. The θ coordinate resembles a specification of latitude, except that is measured down the φ circle from 0° at the zenith, instead of upward from the equator. In the spherical coordinate system, the equator is at $\theta=90^\circ$. All points whose second coordinate θ is 90 lie on the equatorial great circle. With the exception of these, all points with the same θ lie on the same lesser circle and specify a plane along which the dome can be truncated so it will sit flat. The r coordinate, is measured in units of length from the centre, specify how far out a point is to be found. If the points are on the surface of a sphere, like the vertices of a spherical geodesic structure, length r can be assumed as 1 and virtually disregard it. The angles θ and φ tell all is necessary to know about the structure. If the envelope of the system is other than spherical, then varying values of r will have to be taken into account. If we know the coordinates θ_1, φ_1, r_1 and θ_2, φ_2, r_2 of two points, then we can find the distance between them by inserting these values into an equation (1). The unit of d value will be the same as unit of r , and if $r=1$ the result d will be a chord factor.

$$d = \sqrt{2 - 2\{\cos\theta_1\cos\theta_2 + \cos(\varphi_1 - \varphi_2)\sin\theta_1\sin\theta_2\}} \quad (1)$$

Knowing the appropriate values of angles and radius, we can transform the spherical coordinates into the Cartesian system using the formulas:

$$\begin{aligned} x &= r \sin\theta \cos\varphi \\ y &= r \sin\theta \sin\varphi \\ z &= r \cos\theta \end{aligned} \quad (2)$$

This method permits a standardized procedure of coordinate determining. All chord factors are found by exactly the same routine, and all are found independently, errors are isolated, and do not affect other computations. By using a good pocket calculator, which can quickly change angles into their sines and cosines, permits us to run through the chord-factor equation for each pair of points in less than a minute, even when coordinates are cumbersome [3].

3. Mode of stability loss

Stability is the fundamental issue related to the steel building structural system. Structural stability involves the capability of the structure to maintain unchanged position and shape under loads acting on it. As regards steel buildings, stability is crucial importance because of the slenderness of the members. Structures are exposed to a hazard of a sudden occurrence of stability loss when they are subjected to massive compressive loads. The theory of stability deals with the determination of critical load capacity and critical states of the structure, i.e. states, which are accompanied by rapid changes in the form of its deformation or the value of displacements of certain points. In the stability theory, we can distinguish three basic types of loss of stability [4-10]. The first is local buckling in which the critical load capacity of individual bars is exceeded. Geometrical interpretation of buckling length coefficient of compressed bars is shown in figure 3.

The other two modes are related to the concepts of limit and bifurcation points. The structure behaviour associated with the loss of stability at the limit point is called a snap-through.

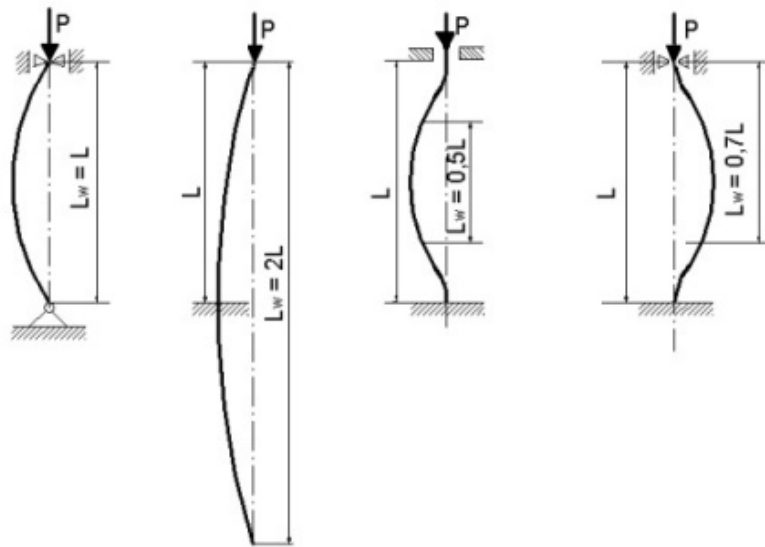


Figure 3. Geometrical interpretation of buckling length of compressed bars.

The example of node snap-through on the simplest lattice structure - Mises truss - presents the real situation that can occur in the lattice domes (figure 4a). In the case the loss of stability occurs at the bifurcation point, the resulting behaviour of the structure is called bifurcation buckling. Two different examples of bifurcation buckle mode: symmetrical and antisymmetrical are presented in figure 4b.

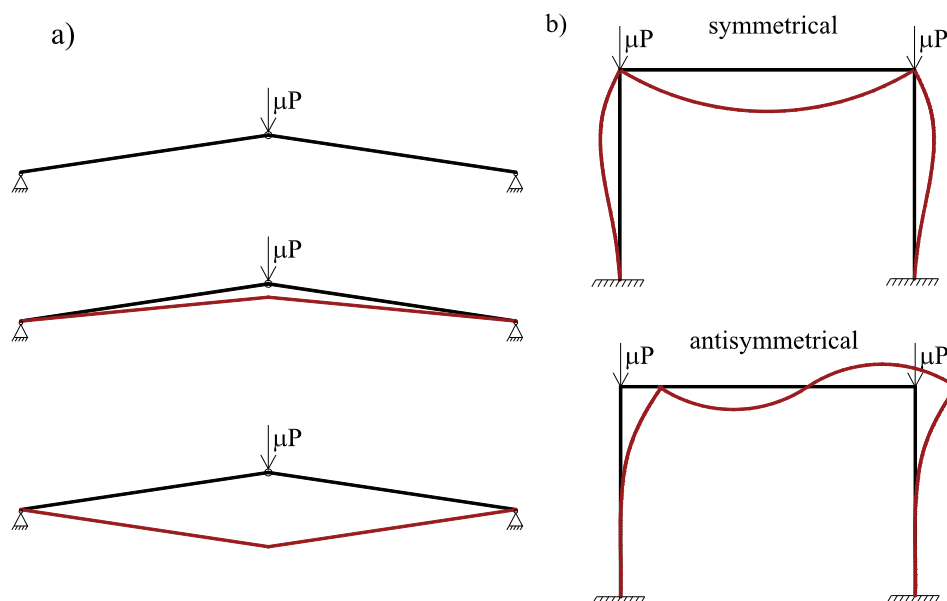


Figure 4. Geometrical interpretation of two different forms loss of stability: a) snap-through, b) bifurcation

To ensure appropriate and safe operation of the structure, i.e. it's being in the state of static equilibrium, the value of equilibrium (critical load capacity) and eigenvectors (buckling modes) must be determined. The stability analysis of bars structures by means of the finite element method involves the solution of large systems of nonlinear equations. In the paper for the solution of nonlinear equation the incremental-iterative method constant arc length is applied [11].

4. Results and discussions

In the paper, two computational models, namely 3V and 4V were taken into consideration. They differ in the frequency of subdivision of spherical triangles. For 4V model, two types of structures, truss and frame ones, were analysed. In each model, the rise is 6,448.253 mm, and span is 20,866.986 mm. The elements of the structure are assumed to be made of RO70x5 steel pipes with yield point $f_y=235$ MPa and Young's modulus $E=210$ GPa. One-parameter nodal load was taken into account. In the analyses, the values of the critical load capacity were determined and the most stressed struts were identified for each case.

3V model represents a geodesic dome composed of 31 nodes and 75 struts (figure 5), and the dome coordinates of nodes are listed in table 1. In 4V model, 51 nodes and 130 struts were generated. They are presented in figure 6, and their geometry - in table 2.

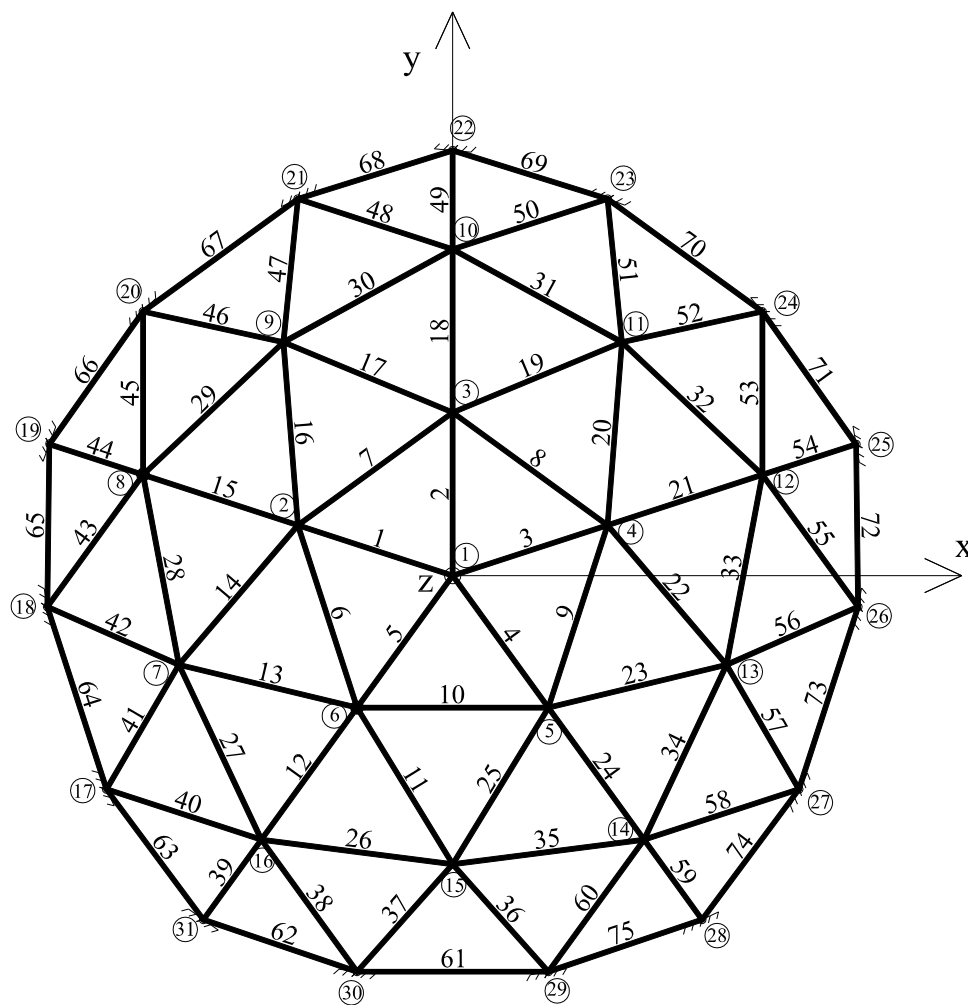


Figure 5. Mesh of the 3V geodesic dome model

Table 1. Geometry of 3V geodesic dome model

No. of node	x [mm]	y [mm]	z [mm]	No. of node	x [mm]	y [mm]	z [mm]
1	0.000	0.000	11665.000	17	-8515.748	-5241.756	6006.518
2	-3808.358	1237.411	10956.160	18	-9970.412	-764.762	6006.518
3	0.000	4004.345	10956.160	19	-9922.842	3224.127	5216.747
4	3808.358	1237.411	10956.160	20	-7616.717	6479.166	6006.518
5	2353.695	-3239.583	10956.160	21	-3808.358	9246.101	6006.518
6	-2353.695	-3239.583	10956.160	22	0.000	10433.493	5216.747
7	-6734.791	-2188.266	9269.644	23	3808.358	9246.101	6006.518
8	-7616.717	2474.821	8481.339	24	7616.717	6479.166	6006.518
9	-4162.330	5728.955	9269.644	25	9922.842	3224.127	5216.747
10	0.000	8008.690	8481.339	26	9970.412	-764.762	6006.518
11	4162.330	5728.955	9269.644	27	8515.748	-5241.756	6006.518
12	7616.717	2474.821	8481.339	28	6132.653	-8440.873	5216.747
13	6734.791	-2188.266	9269.644	29	2353.695	-9718.749	6006.518
14	4707.390	-6479.166	8481.339	30	-2353.695	-9718.749	6006.518
15	0.000	-7081.378	9269.644	31	-6132.653	-8440.873	5216.747
16	-4707.390	-6479.166	8481.339				

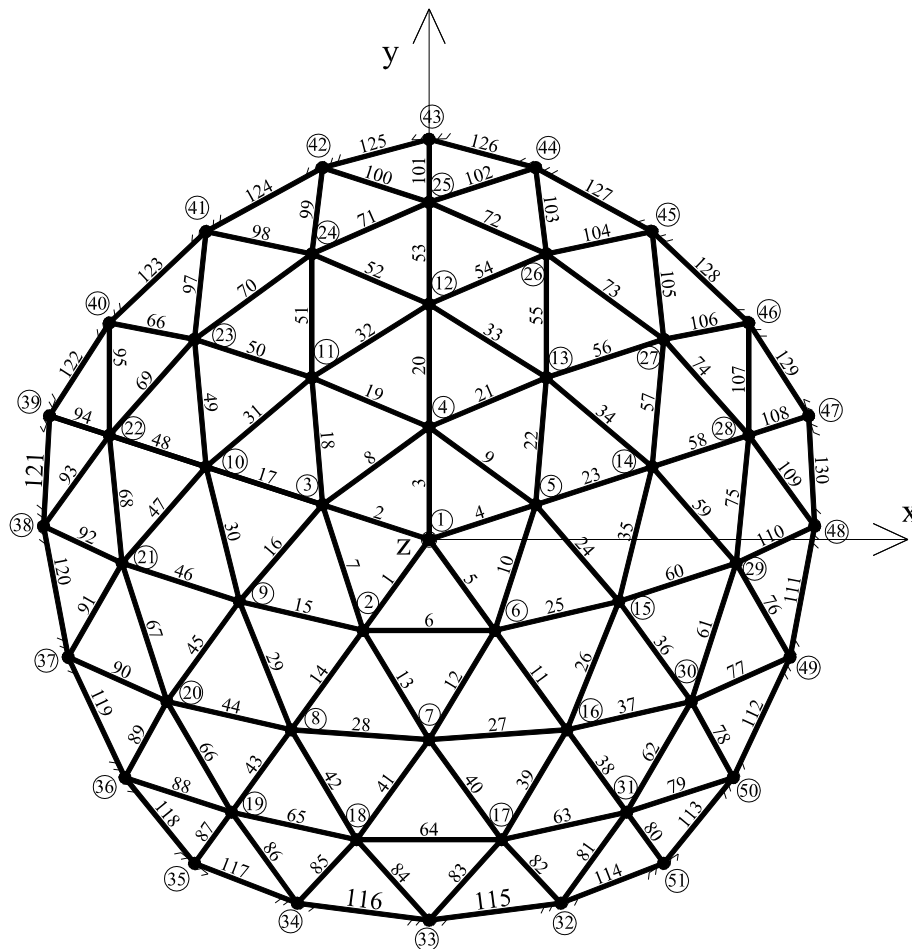
**Figure 6.** Mesh of the 4V geodesic dome model

Table 2. Geometry of 4V geodesic dome model

No. of node	x [mm]	y [mm]	z [mm]	No. of node	x [mm]	y [mm]	z [mm]
1	0.000	0.000	11665.000	27	6132.653	5216.747	8440.873
2	-1721.998	-2370.127	11291.122	28	8358.753	2715.924	7669.891
3	-2786.251	905.308	11291.122	29	8027.748	-615.753	8440.873
4	0.000	2929.638	11291.122	30	6856.515	-4220.437	8440.873
5	2786.251	905.308	11291.122	31	5165.994	-7110.380	7669.891
6	1721.998	-2370.127	11291.122	32	3443.996	-9480.507	5859.276
7	0.000	-5216.747	10433.493	33	0.000	-9922.842	6132.653
8	-3604.683	-4961.421	9922.842	34	-3443.996	-9480.507	5859.276
9	-4961.421	-1612.063	10433.493	35	-6132.653	-8440.873	5216.747
10	-5832.500	1895.094	9922.842	36	-7952.245	-6205.072	5859.276
11	-3066.327	4220.437	10433.493	37	-9437.183	-3066.327	6132.653
12	0.000	6132.653	9922.842	38	-10080.751	345.797	5859.276
13	3066.327	4220.437	10433.493	39	-9922.842	3224.127	5216.747
14	5832.500	1895.094	9922.842	40	-8358.753	5645.561	5859.276
15	4961.421	-1612.063	10433.493	41	-5832.500	8027.748	6132.653
16	3604.683	-4961.421	9922.842	42	-2786.251	9694.221	5859.276
17	1895.094	-7825.120	8440.873	43	0.000	10433.493	5216.747
18	-1895.094	-7825.120	8440.873	44	2786.251	9694.221	5859.276
19	-5165.994	-7110.380	7669.891	45	5832.500	8027.748	6132.653
20	-6856.515	-4220.437	8440.873	46	8358.753	5645.561	5859.276
21	-8027.748	-615.753	8440.873	47	9922.842	3224.127	5216.747
22	-8358.753	2715.924	7669.891	48	10080.751	345.797	5859.276
23	-6132.653	5216.747	8440.873	49	9437.183	-3066.327	6132.653
24	-3066.327	7444.563	8440.873	50	7952.245	-6205.072	5859.276
25	0.000	8788.913	7669.891	51	6132.653	-8440.873	5216.747
26	3066.327	7444.563	8440.873				

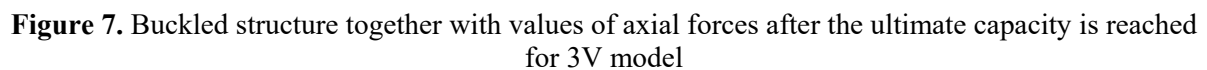
4.1. 3V geodesic dome – truss model

The first case considered in the paper is frequency (3V) geodesic dome, modelled as a truss structure. Two types of analyses were conducted, namely linear buckling and non-linear statics [1]. Capacities of individual struts were verified. The results of individual analyses are shown in table 3.

Table 3. Results of analysis for 3V geodesic dome model

	Linear buckling	Nonlinear statics	Nonlinear statics when bar capacity is taken into account
Limit value of load multiplier	2887.24	1629.12	36.81

As regards 3V geodesic dome, the most stressed struts are those no. 12, 15, 18, 21 and 24. The analyses carried out for the study showed that a decisive mode of stability loss is local buckling of struts, whereas a global mode of stability loss is snap-through of the nodes. Buckled structure form, together with values of axial forces after the ultimate capacity of the struts is reached can be seen in figure 7.



The second example concerns 4Vgeodesic dome that was modelled as a truss structure. The same analyses were conducted as for case 4.1, and the results are listed in table 4.

	Linear buckling	Nonlinear statics	Nonlinear statics when bar capacity is taken into account
Limit value of load multiplier	1097.45	412.30	45.46

8

4.3. 4V geodesic dome–frame model

In the last example, 4V geodesic dome was modelled as a frame structure. The analyses were conducted in the same way as for two previous cases. The results are compiled in table 5.

Table 5. Results of analysis for 4V geodesic dome frame model

	Linear buckling	Nonlinear statics	Nonlinear statics when bar capacity is taken into account
Limit value of load multiplier	92.60	93.22	44.96

The analysis showed that for the frame model, local buckling of struts is again a dominant mode of stability loss. However, the mode of global stability loss is changed and it occurs by bifurcation point of the equilibrium path. In this model, struts no. 38, 43, 48, 53 and 58 are the most stressed ones. Buckled structure form, and values of axial forces after the ultimate capacity of the struts is reached are presented in figure 9.

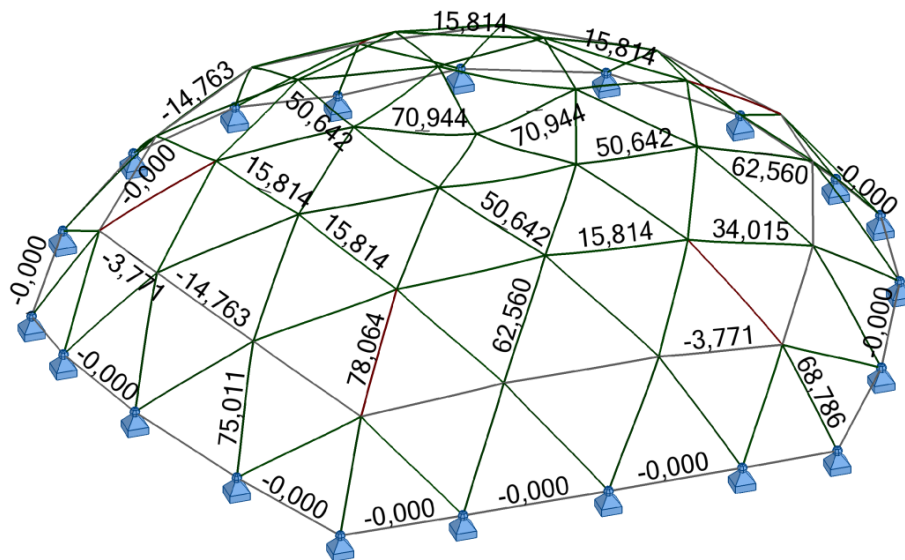


Figure 9. Values of axial forces after the limit load is reached for the 4V frame model

It should be added that to conduct analysis with Robot Structural Analysis program, it is necessary to account for the strut type and appropriate buckling length coefficients related to the stiffness of the restraint. In the case above, the default value of the buckling length coefficient $\mu=1.0$ was analysed. To better illustrate the impact of coefficient μ on the capacity of the structure, the same analyses were made for two other options offered by the program μ : 0.5 and 0.7. The coefficient values significantly affect a change in the limit capacity of the struts, the respective values are 77.82 kN for $\mu=0.7$, and 91.80 kN for $\mu=0.5$. Subsequent papers will focus on the determination of the accurate stiffness of the connection and the buckling length coefficient.

5. Conclusions

In the paper, the effect produced by an increase in the density of nodes in the geodesic dome on the structure limit capacity was discussed. Two computational models were considered, namely 3V and 4V, which differ in the density of nodes. Additionally, for 4V model, two types of strut connections in the nodes were verified.

Due to the height-to-span ratio of 0.309, the structure of concern is classified as high-rise dome. Buckling of bars was found to be a decisive mode of local stability loss in all models. Global modes of stability loss differ in cases 4.1-4.2 than 4.3. For the structures modelled as spatial trusses, node snap-

through is the global mode of stability loss, whereas for the frame structure, it is the bifurcation of the equilibrium path. It should be added that even when the structure is modelled taking into account bar buckling coefficient $\mu=0.5$, which corresponds to a rigid connection, the local or global modes of stability loss do not change.

The effect of single-layer shallow lattice dome modelling on the critical load capacity was discussed in paper [12].

References

- [1] J. Bródka, A. Kozłowski, "Design and computations of joints and nodes of steel structures" (in Polish), *PWT*, **T.1**, 2013.
- [2] www.chodor-projekt.pl (accessed 28.03.2018).
- [3] H. Kenner, "Geodesic math and how to use it", *University of California*, 1976.
- [4] J. Marcinowski, „Stability of elastic structures” (in Polish), *Dolnośląskie Wydawnictwo Edukacyjne*, 2017.
- [5] Z. Waszczyszyn, Cz. Cichoń, M. Radwańska, "Stability of Structures by Finite Element Methods", *Elsevier*, 1994.
- [6] P. Obara, J. Kłosowska, W. Gilewski, "Form finding of tensegrity structures via Singular Value Decomposition of compability matrix", *Advances in mechanics: Theoretical, Computational and Interdisciplinary Issues*, Taylor & Francis Group, London, pp. 191-195, 2016.
- [7] P. Obara, J. Kłosowska, J. Turant, "Kinematically admissible failure mechanisms for plane trusses", *IOP Conf. Series: Materials Science and Engineering* 245, DOI:10.1088/1757-899X/245/2/022022, 2017.
- [8] W. Mochocki, P. Obara, U. Radoń, P. Zabojszcza, "Effect of single-layer truss dome geometry on critical load capacity", *Structure and Environmental*, **Vol. 93**/2017, pp. 152-164, 2017.
- [9] U. Pawlak, M. Szczecina, "Dynamic eigenvalue of concrete slab road surface", *IOP Conf. Series: Materials Science and Engineering* 245, DOI:10.1088/1757-899X/245/2/022022, 2017.
- [10] U. Pawlak, M. Pawlak, "Type of material in the pipes overhead power lines impact on the distribution on the size of the overhang and the tension", *IOP Conf. Series: Materials Science and Engineering* 245, DOI:10.1088/1757-899X/245/2/022022, 2017.
- [11] E. Riks, "An incremental approach to the solution of snapping and buckling problems", *Int. J. Solids Struct.* **15**, , pp. 529-551, 1979.
- [12] P. Zabojszcza, U. Radoń, P. Obara, "Impact of single-layer dome modelling on the critical load capacity", *Matec Web of Conferences* (in press), 2018